Negative density dependence promotes persistence of a globally rare yet locally abundant plant species *(Oenothera coloradensis)*

Abstract

Identifying the mechanisms underlying the persistence of rare species has long been a motivating question for ecologists. Classical theory implies that community dynamics should be driven by common species, and that natural selection should not allow small populations of rare species to persist. Yet, a majority of the species found on Earth are rare. Consequently, several mechanisms have been proposed to explain their persistence, including negative density dependence, demographic compensation, vital rate buffering, asynchronous responses of subpopulations to environmental heterogeneity, and fine-scale source-sink dynamics. Persistence of seeds in a seed bank, which is often ignored in models of population dynamics, can also buffer small populations against collapse. We used integral projection models (IPMs) to examine the population dynamics of *Oenothera coloradensis*, a rare, monocarpic perennial forb, and determine whether any of five proposed demographic mechanisms for rare species persistence contribute to the long-term viability of two populations. We also evaluate how including a discrete seed bank stage changes these population models. Including a seed bank stage in population models had a significantly increased modeled *O. coloradensis* population growth rate. Using this structured population model, we found that negative density- dependence was the only supported mechanism for the persistence of this rare species. We propose that high micro-site abundances within a spatially heterogeneous environment enables this species to persist, allowing it to sidestep the demographic and genetic challenges of small population size that rare species typically face. The five mechanisms of persistence explored in our study have been demonstrated as effective strategies in other species, and the fact that only one of them had strong support here supports the idea that globally rare species can employ distinct persistence

strategies. This reinforces the need for customized management and conservation strategies that mirror the diversity of mechanisms that allow rare species persistence.

Introduction

Determining how and why populations of rare species persist has been a goal for ecologists since the discipline's inception (Drury, 1974; Levins & Culver, 1971). Theoretically, low population size is a final step on a trajectory toward extinction (Rosenzweig & Lomolino, 1997; Stanley, 1979) or the first step toward ubiquity (Spear et al., 2021). Yet, small but stable populations of rare species exist in every ecosystem and taxonomic group (Magurran & Henderson, 2011). In fact, a large proportion of species globally – as many as 35% of plant species, for example— can be considered naturally rare (Enquist et al., 2019). The prevalence of rarity suggests it is an evolutionarily stable strategy rather than a stop along the path toward extinction or invasion, and implies that there must be both fundamental and realized niches that are available for rare species to occupy. A growing body of evidence demonstrates the importance of rare species for biological processes, including their impacts on community stability (Arnoldi et al., 2019; Säterberg et al., 2019), and functional composition (Burner et al., 2022; Leitão et al., 2016), which in turn impact ecosystem function (Lyons et al., 2005).

Effective conservation and management of rare species require an understanding of both the conditions causing rarity initially, and the mechanisms that allow rare species to persist. Causes of rarity can vary from highly-specific habitat requirements (Sgarbi & Melo, 2018), to adverse impacts of anthropogenic environmental change (Vincent et al., 2020). To then persist in a state of rarity, a species must overcome any of multiple potential challenges, primarily the negative effects of demographic, environmental, and genetic stochasticity, defined as random variation in vital rates (e.g., survival, reproduction), abiotic conditions, or genetic allele frequencies (May,

1973). Stochastic deleterious events can cause extirpation or even extinction of rare species, since there may not be enough unaffected individuals or subpopulations to "rescue" the affected population (Nei et al., 1975). Rare species that maintain populations over time typically do so by employing demographic strategies that compensate for the adverse effects of small population size. There are five strategies that have been most-commonly advanced in the literature that allow persistence of rare populations (Fig. 1) (Dibner et al., 2019): negative density-dependence (Rovere & Fox, 2019), demographic compensation (Villellas et al., 2015), vital rate buffering (Hilde et al., 2020; Pfister, 1998), asynchronous responses between subpopulations (Abbott et al., 2017), and fine-scale source-sink dynamics (Kauffman et al., 2004; Pulliam, 2016). Negative density-dependence occurs when the growth rate (λ) of a population increases at small population size. With this mechanism, intraspecific competition decreases at low densities, which then benefits surviving individuals and reduce the likelihood of extirpation. Demographic compensation occurs when different vital rates are affected in opposing ways by the same perturbation in the environment, which can help maintain a relatively constant population λ in response to environmental variation. Vital rate buffering occurs when the variability of vital rates decreases as the vital rate becomes more important for population growth rate (i.e., the vital rate has a higher elasticity), which prevents the negative effects of temporal variation on the deterministic λ across time (Tuljapurkar, 1989). Spatial asynchrony occurs when subpopulations close to one another have different or even opposing growth rates, resulting in a stable population-wide λ. Fine-scale source-sink dynamics occur when there is exchange of individuals between subpopulations that bolsters the size and genetic diversity of very small subpopulations, which again results in a stable population-level λ. Each of these mechanisms can act independently, but also can interact or overlap (Dibner et al., 2019).

Here, we consider this suite of persistence mechanisms, and identify which contribute to the persistence or population growth of a rare, endemic plant species, *Oenothera coloradensis* (Rydberg) W.L. Wagner & Hoch (Onagraceae). We use demographic data from three consecutive years of observational field study, which allows us to test for the presence of a mechanism directly in four cases, and to test for pre-requisite underlying conditions in the fifth case. We use integral projection models (IPMs) (Easterling et al., 2000) that include a discrete seed bank population state. IPMs are flexible models of population dynamics that are constructed using regression models that describe vital rate change across a continuous state variable such as size. IPMs have multiple advantages including better performance with small datasets than traditional matrix models (Ramula et al., 2009), and the ability to directly incorporate covariates of interest directly into vital rate models. We built these models with two objectives in mind.

Our first objective was to determine if including information about the seed bank significantly altered population models for *O. coloradensis*. Seed banks can serve as important reservoirs of genetic diversity and buffer populations against collapse (Jongejans et al., 2006; Vitalis et al., 2004), and can be especially critical for monocarpic perennials such as *O. coloradensis* that only flower once in their lifetime (Rees et al., 2006). For these reasons, we expected that a soil seed bank is important for long-term persistence of *O. coloradensis* populations. Seed banks are often not included in population models because their parameters can be very difficult to estimate, but previous work shows that including them can significantly alter model outcomes (Nguyen et al., 2019; Paniw et al., 2017). We predicted that including a discrete seed bank state in IPMs would increase the λ for *O. coloradensis* populations, demonstrating that seed banks are important for maintaining the population in the long term.

Our second objective was to identify whether any of the five aforementioned persistence mechanisms was acting to maintain *O. coloradensis* populations. Whereas a seedbank can serve as a reservoir of individuals within a population that can prevent extirpation, these five persistence mechanisms represent demographic strategies that the population utilizes to persist. This species occurs in habitats that naturally experience frequent, highly localized disturbance, meaning that some subpopulations might be negatively affected by flood, for example, while other nearby subpopulations are simultaneously thriving due to lack of disturbance. Additionally, previous matrix population models constructed for this species in the 1990s found substantial variation in λ across space and time (Floyd & Ranker, 1998). The population-wide pattern of asynchronous habitat disturbance also could make source-sink dynamics important. Finally, we have evidence of large fluctuations in the number of plants within subpopulations (Heidel et al., 2021), which suggest that population growth rate decreases at high population size and increases at low population size. Therefore, we predicted that density dependence, small-scale source-sink dynamics and asynchronous responses between subpopulations would be important mechanisms of persistence for *O. coloradensis*. This objective contributes to our understanding of this specific species' natural history, but also enhances our collective understanding of persistence strategies in rare species.

Materials and Methods

Species Description

Oenothera coloradensis (Onagraceae) (Wagner et al., 2013) is an herbaceous, monocarpic perennial plant species that primarily occurs in frequently disturbed, mesic or wet meadows, and riparian floodplains (Fertig, 2000). Non-reproductive individuals consist of a rosette of leaves

with a fleshy taproot. Flowering typically occurs after several years, when individuals bolt and produce a 10-30 cm long floral stalk. Individuals typically die after reproducing–93% of the time in populations we observed. Frequent disturbance such as flooding that reduces growth of both woody and herbaceous species and removes litter is important for this species, especially for successful seedling recruitment (Burgess, 2003; Fertig, 2000). *O. coloradensis* is an obligate-out crosser pollinated primarily by hawkmoths (Krakos, pers. comm. to B. Heidel, 2013). Seed dispersal occurs by gravity around parent plants, and by water in sporadic flood events (Heidel et al., 2021)**.**

All historical and known extant *O. coloradensis* populations lie within a 7,000-hectare area that includes southeast Wyoming, northern Colorado, and a small part of southwest Nebraska **(Fig. 2)**. The only known population on Federal land occurs on the F. E. Warren Air Force Base near Cheyenne, WY (FEWAFB). The Soapstone Prairie Natural Area (Soapstone), owned by the city of Fort Collins, CO, has the largest known population of *O. coloradensis* individuals (Heidel et al., 2021). Decline in a majority of the known populations between the mid-1980s and 2000 lead the U.S. Fish and Wildlife Service (USFWS) to designate *O. coloradensis* as a "threatened" species protected under the Endangered Species Act in 2000 (U.S. Fish and Wildlife Service, 2000). Although this species appears to be naturally rare, mangers were concerned that habitat loss due to ranching, natural resource extraction, and shrub encroachment may lead to extinction of this species. However, based on additional monitoring following the initial listing decision, the USFWS determined that *O. coloradensis* populations exhibit considerable natural variation in size, and that while monitored populations have both increased and decreased since the initial listing decision, the species as a whole does not appear to be on a trajectory toward extinction. As a result, *O. coloradensis* was de-listed in 2019 (U.S. Fish and Wildlife Service, 2019).

Previous work established that *O. coloradensis* population growth rate is particularly impacted by recruitment of seedlings (Floyd & Ranker, 1998). Seed banks are also likely important, since years of high seedling density are not necessarily preceded by years of high rates of flowering and seed production (Heidel et al., 2021; Munk et al., 2002). The *O. coloradensis* seed bank has not been studied directly, but a greenhouse seed study showed that an average of 58% of seeds produced by a parent plant are viable, and that a viable seed has a 20% probability of germinating after two months of cold stratification. These rates did not change meaningfully over five years. More information about *O. coloradensis* can be found in the Supporting Information.

Demographic Data Collection

We conducted a three-year demographic study of *O. coloradensis* across six spatially distinct subpopulations, three in the FEWAFB population and three at the Soapstone population ("Unnamed creek", "Crow creek", and "Diamond creek" at FEWAFB and "Meadow", "HQ3" and "HQ5" at Soapstone)(Table S1; Fig. 2**)**. In early summer 2018, we established three 2x2 m^2 quadrats in each of these subpopulations, resulting in 18 plots (Table S1). Plants larger than 3 cm are typically non-seedling plants at least one year in age. In each study plot, we tagged and mapped each unique non-seedling individual and recorded longest leaf length, reproductive status (bolting and/or flowering), and seed production for each. Individuals smaller than 3 cm in leaf length are typically seedlings that germinated that year, occur at high density, and are less likely to survive than non-seedling plants. Due to these factors, we tallied seedlings in each plot, but did not map or tag them. In subsequent 2019 and 2020 censuses, we mapped and tagged new non-seedling individuals, and re-measured all surviving individuals from previous years. Sample size in a given year at a subpopulation ranged from 48 to 1527 individuals (Table S1). All mapping, tagging, and leaf measurements took place between late May and early July, during the

peak of vegetative growth for this species. We conducted a second round of site visits in early fall at the end of flowering, during which we confirmed that plants designated as "reproductive" during the summer census did in flower, and collected data on seed production.

It was not possible to measure seed production exactly because *O. coloradensis* seeds are contained in indehiscent capsules. Additionally, buds on the same individual flower and set seed with a time lag of up to several weeks, so mature seed capsules often exist at the tip of a stem while unopened buds lower down on that same stem have not yet flowered. This lag makes it difficult to count the total number of capsules produced by an individual. However, seed capsules leave a noticeable scar on the stem after they fall, so we used the number of seed capsule scars present on reproductive stems as an estimate of capsule production. Counting scars is extremely time-intensive since a single plant can produce several hundred capsules, so we used Poisson generalized linear regression to estimate the relationship between the length of stem bearing capsule scars and the number of capsules produced by that stem. A Poisson generalized linear regression model fit to stem measurements and capsule counts from 106 individuals in 2018 indicated that the number of capsules produced by an individual (C) can be predicted by $\exp(1.843 + 0.119S)$, where S is the stem length in cm (pseudo $R^2 = 0.42$, $P < 0.01$, Residual deviance = 186.98, df = 104) (Fig. S1). We used this relationship to estimate capsule production for each reproductive individual. Previous work indicated that each capsule contained an average of 4 seeds, so we multiplied the estimated number of capsules produced by an adult plant by 4 to estimate seed production (Burgess et al., 2005). Finally, we conducted *in-situ* and lab-based experiments to estimate seed germination rate, the rate of decline in seed viability over time, and the size of the seed bank. More information about this data collection can be found in the Supporting Information.

Environmental Measurements

To determine the effect of temporal variation in climate on *O. coloradensis* population persistence strategies, we used modeled, population-level temperature and precipitation data from PRISM (PRISM Climate Group; Oregon State University, 2021), which we refer to as "environmental covariates". We calculated mean growing season temperature, mean temperature during the preceding winter, total water-year precipitation (from October in the previous year to September in the current year), and the standard deviation of each of these metrics for each year of vital rate data collection at FEWAFB and Soapstone Prairie. We used water-year precipitation because the shortgrass steppe receives a majority of its annual precipitation in the form of snow, and melting snow from the previous winter likely drives springtime seedling recruitment. Average temperature of the previous winter is also likely important for seedling recruitment, because seed germination is triggered by cold stratification (Burgess et al., 2005). Growing season temperature and precipitation are likely important for growth, survival, and reproductive output of non-seedling plants.

Vital Rate Models

We used data from the three-year demographic monitoring study detailed above to parameterize models of *O. coloradensis* vital rates (shown in Fig. 3; parameters of fitted vital rate functions are shown in Table S2). We first estimated continuous vital rate functions describing how survival probability, growth, flowering probability, and seed production in year $t+1$ each vary as a function of longest leaf size in year t. We also initially included a quadratic term for longest leaf size in year t in these models, but AIC model selection determined that this term only improved models for flowering probability. We also estimated the distribution of new recruit size in year $t+1$. Finally, we estimated discrete vital rate parameters describing the probability of

seeds produced in year *t* either entering the seed bank or germinating in year *t+1*, as well as the probability of seeds in the seed bank in year *t* either staying in the seed bank or germinating in year *t+1*.

We first created global models for each continuous vital rate, which are described in detail in the Supporting Information (Table. 1). We then used these global model structures to fit different versions of these continuous vital rate functions, each of which described vital rate processes at different temporal and spatial scales. Models were fit using data from the first transition (2018-2019), the second transition (2019-2020), or pooled across both transitions. We also made models using data from a single subpopulation, a single population, or pooled across both populations. We additionally fit models that expanded on the global model structures by including density dependence terms and/or environmental covariates (total or standard deviation of water year precipitation, mean or standard deviation of annual growing season temperature, or mean or standard deviation of annual winter temperature). When density dependence or environmental covariates were included, we used AIC model selection to confirm that including these covariates improved model fit.

All continuous vital rate models, regardless of scale, were parameterized using data from non-seedling plants as well as seedlings. Although seedlings (above-ground plants < 3 cm in leaf length) were only tallied in each plot quadrant and year instead of tagged and measured, we incorporated them into the dataset for continuous, above-ground plants by assigning them a random size drawn from a continuous, uniform probability distribution (seedling size $\sim U(0.1, 3)$). Each new recruit to the > 3 cm stage in year *t+1* was randomly assigned to a seedling within the same plot quadrant in year *t*. Seedlings in year *t* that were assigned a recruit in year *t+1*

survived, while those without an assigned recruit died. Incorporating seedlings into the continuous dataset in this fashion allowed us to create IPMs using only one discrete stage.

We estimated discrete vital rates for seeds uniformly across both populations and years, using data we collected in conjunction with previously published germination and viability data (Table 1). We did not have the data required to determine how these rates changed across subpopulations or in response to abiotic variation, due to the difficulties of estimating *in situ* seed germination and death. We used the following parameters to estimate discrete seed vital rate parameters: viable seed germination rate (germ. rate) = 0.16, viability rate of seeds produced by a parent plant (viab. rate) = 0.58, rate of natural seed death in the seed bank (death rate) = 0.10. More information can be found in the Supporting Information.

Population Models

We used estimates of discrete and continuous *O. coloradensis* vital rates, detailed above, to parameterize a suite of integral projection models (IPMs) for *O. coloradensis*. We then used these models to address each of the objectives outlined in the Introduction.

Objective 1: Quantifying the Importance of the Seed Bank Stage: We used two different IPMs to determine whether explicitly including a discrete seed bank stage in a population model leads to significantly different outcomes relative to a model without a seed bank stage. We first created a density-independent IPM using continuous vital rate functions parameterized with data from both Soapstone and FEWAFB. This model had a single continuous, size-based population state, and did not include a seed bank state (Table 2: IPM "A"; Eqn. 1). This IPM used a kernel structure where the continuous, above-ground population state ($n(z',t+1)$) at time $t+1$ was described by the following equation:

Equation 1

$$n(z', t+1) = \int_L^U (1 - Pb(z))s(z)G(z', z)n(z, t)dz + pEstab \int_L^U Pb(z)b(z)co(z')n(z, t)dz$$

Then, we created an IPM that included both a discrete seed bank state, and a continuous, size-based stage for above-ground individuals (Table 2: IPM "B"; Eqns. 2 & 3) (Ellner & Rees, 2006; Paniw et al., 2017; Rees et al., 2006). This model used the same continuous vital rate functions as in IPM A, but also included discrete probabilities describing the probabilities of seeds produced in year *t* germinating or going into the seeds bank in year *t+1*, as well as probabilities of seeds in the seed bank in year *t* germinating or persisting in the seed bank in year *t+1*. This IPM with two population states used a kernel structure where the continuous, above-ground population state (n(*z*',*t+1*)) and the seed bank state (B(*t+1*)) at time *t+1* were described by the following equations:

Equation 2

$$n(z', t+1) = \int_L^U (1 - Pb(z))s(z)G(z', z)n(z, t)dz + goCont \int_L^U Pb(z)b(z)co(z')n(z, t)dz + outSB$$

Equation 3

$$B(t+1) = goSB \int_L^U Pb(z)b(z)n(z, t)dz + B(t)staySB$$

In equations for both types of IPMs, *z* is the distribution of plant longest leaf size (measured as longest leaf length) in the current year ("size$_t$"), z' is the distribution of plant longest leaf size in the next year ("size$_{t+1}$"), and U and L are the upper and lower boundaries of leaf size. G(*z*', *z*) is the vital rate function describing \$size$_{t+1}$ as a function of size$_t$ (Table 1). The vital rate functions *s*(*z*), *Pb*(*z*), and *b*(*z*) describe the relationship between size$_t$ and survival probability of non-flowering plants, flowering probability, and seed production of flowering plants, respectively. c_o(*z*') is the distribution of above-ground recruit size$_t$. *goCont*, *outSB*, *goSB*, and *staySB* are discrete parameters that determine seed bank dynamics. *goCont* is the probability of a seed

produced in year$_t$ germinating as a seedling in year$_{t+1}$, *outSB* is the probability of a seed from the seed bank in year$_t$ germinating as a seedling in year$_{t+1}$, *goSB* is the probability of a seed produced in year$_t$ going into the seed bank in year$_{t+1}$, and *staySB* is the probability of a seed from the seed bank in year$_t$ persisting in the seed bank in year$_{t+1}$ (Paniw et al., 2017). *pEstab* is the probability of a seed produced in year$_t$ establishing as a seedling in year$_{t+1}$, and is only used in the IPM with no seedbank stage.

We used these vital rate functions and discrete parameters described above to construct discretized IPM kernels for IPM "A" and IPM "B". All kernels were numerically implemented using the “midpoint rule” method (Easterling et al., 2000) with 500 bins, an upper size limit corresponding to 120% of the maximum observed longest leaf size and a lower size limit corresponding to 80% of the minimum simulated seedling size of 0.1 cm. We corrected for eviction following methods from (Williams et al., 2012). We then used eigen analysis of these kernels to estimate asymptotic population growth rate (λ), damping ratio, stable size distribution, and reproductive value (Caswell, 2001; Ellner et al., 2016). We used 1000 iterations of nonparametric bootstrap resampling to estimate 95% bootstrap confidence intervals (95% CIs) for each continuous vital rate parameter included in each IPM, as well as each estimate of λ (Fieberg et al., 2020; Merow et al., 2014). We were unable to estimate CIs for discrete seed bank parameters because they were, in part, drawn from a previous publication. We used perturbation analysis to determine the sensitivity and elasticity of λ to changes in germination rate, viability rate, seed survival rate, and each continuous vital rate model (Morris & Doak, 2002). Finally, to determine whether including a discrete seed bank state significantly altered our population model, we compared the asymptotic λ and associated 95% CI between IPM "A" and IPM "B."

Objective 2: Evaluating Persistence Mechanisms

297 To evaluate whether any of the demographic mechanisms of rare species persistence outlined in
298 Fig. 1 are acting in populations of *O. coloradensis*, we fit a series of IPMs that each used
299 different subsets of data and/or additional covariates in vital rate functions (Table 2: IPMs "C" –
300 "NN"). These IPMs all had a mathematical form equivalent to that of IPM "B" described above,
301 with a discrete seed bank state, and a continuous, size-based stage for above-ground individuals
302 (Eqns. 2 & 3). We then used each of these IPMs, as well as the vital rate functions used to
303 construct them, to evaluate a different persistence mechanism. Details of this process for each
304 persistence mechanism are provided below. It is important to note that, although we use "λ" to
305 refer to population growth rate throughout the text, this value was calculated in slightly different
306 ways depending on the type of IPM. For IPMs without density dependence or environmental
307 covariates, we calculated asymptotic growth rate ($\ln(\lambda_a)$) using eigen analysis of the transition
308 matrix (as described above for IPMs "A" and "B"). For IPMs that used vital rate models with
309 coefficients for density dependence or environmental covariates, we used the ipmr R package to
310 determine stochastic growth rate ($\ln(\lambda_s)$) through iteration (Levin et al., 2021). Although we
311 include these $\ln(\lambda_s)$) values in the Table 2 for interpretation, it is important to note that only the
312 vital rate models, not $\ln(\lambda_s)$ values, from these IPMs were used in tests to evaluate persistence
313 mechanisms.

314 Negative Density Dependence*:* In order to determine the importance of density dependence in *O.*
315 *coloradensis* subpopulations, we used IPMs and vital rate functions that were fit uniquely for
316 each subpopulation using data from both transitions. However, one set of IPMs included
317 population size in the current year in vital rate models, while another set of IPMs did not
318 (density-independent IPMs: "C"-"H" in Table 2; density-dependent IPMs: "I"-"N"). We used
319 AIC to identify significant differences between vital rate models with and without density

dependence terms. We also used results from subpopulation-level IPMs that did not include covariates for density dependence (Table 2: IPMs "CC"-"NN") for each transition to identify relationships between subpopulation size in year t and ln(λ) (as in Fig. 1), as well as subpopulation size in year t and the ratio of population size in year $t+1$ and subpopulation size in year t. In addition to population size information and ln(λ) values from our IPMs, we also used population sizes and ln(λ) values from a previously-published demographic study of *O. coloradensis* at the three FEWAFB subpopulations that we also monitored (Floyd & Ranker, 1998). A negative relationship between population size in year t and either ln(λ) or the ratio of population size in year $t + 1$ to population size in year t would provide evidence for negative density dependence. Additionally, significant differences between models with and without population size predictor terms would constitute evidence for density dependence.

Demographic Compensation*:* To test for demographic compensation, we calculated the correlation between environmental covariate coefficients in different vital rate models. For this correlation analysis we used vital rate models that were fit using data from each subpopulation and both transitions, and that included covariates for density dependence and as well as environmental covariates that improved model fit (vital rate models from IPMs “S”-“X” in Table 2). A negative correlation between coefficients of the same covariate in different vital rate models would indicate that demographic compensation was taking place (Dibner et al., 2019; Villellas et al., 2015). For example, if soil moisture had a positive effect on growth but a negative effect on survival, this would be evidence for demographic compensation. We tested the significance of negative correlations between environmental covariate coefficients using a randomization procedure adapted from those used in Villellas et al. (2015) and Dibner (2019), where we randomly assigned an environmental covariate coefficient drawn from the observed

distribution of values for that coefficient to each vital rate function, calculated a Spearman correlation matrix between those coefficients in each vital rate function, and counted the number of negative and positive correlations in that matrix. This procedure was repeated 10,000 times to generate null distributions of the expected number of either negative or positive correlations between environmental coefficients that would occur randomly. We compared the observed number of negative or positive correlations between each environmental covariate coefficient to these expected distributions of random correlations to determine statistical significance. We could not test for demographic compensation in discrete seed bank vital rate parameters because we did not know how they varied according to environmental conditions. Either more negative correlations or fewer positive correlations between environmental covariate coefficients in different vital rate models than expected according to the simulated null distribution would provide evidence for demographic compensation (Fig. 1) (Villellas et al., 2015). We conducted this test for demographic compensation using vital rate coefficients for mean growing season temperature, since it was the only environmental covariate that was significant across all vital rate models and did not result in over-fitting. Although we conducted this analysis using coefficients fit to data from only two transitions we were able to compare across six sub-populations, which make our sample size consistent with multiple similar analyses (Villellas et al., 2015).

Vital Rate Buffering*:* We tested for the presence of vital rate buffering in *O. coloradensis* populations by comparing the variability of vital rates to their importance. We used an approach that scales both the standard deviation (variability metric) and sensitivity (importance metric) of vital rates, allowing for a fair comparison of variability and importance across vital rates with fundamentally different relationships between their mean and variance (McDonald et al., 2017).

Vital rates that are probabilities (i.e. survival, flowering, growth, discrete seed bank transition probabilities, and seedling size) are constrained between zero and one and thus typically have small variance as the mean approaches these limits, while other vital rates are only constrained by zero and thus typically have variances that increase as the mean increases (i.e. seed productivity) (Gaillard & Yoccoz, 2003). To enable a fair comparison between these different categories of vital rates, we calculated the importance and variability of probability and non-probability vital rates in different ways. The importance of probability vital rates was defined as the logit variance stabilized sensitivity, and the variability was defined by the standard deviation of the logit transformed vital rate values (McDonald et al., 2017; William A Link, Paul F Doherty, Fr., 2002). The importance of non-probability vital rates was defined as the log-scaled sensitivity (or elasticity), and the variability was defined by the standard deviation of the log-transformed vital rate values (McDonald et al., 2017; Morris & Doak, 2002).

We used an IPM that was fit across all subpopulations using data from both transitions (Table 2: IPM "B") to calculate elasticity or logit VSS values for each discrete vital rate and continuous vital rate function. We calculated the scaled standard deviation for each continuous vital rate function using the vital rates that were fit uniquely for each subpopulation and each transition (Table 2: IPMs "CC"-"NN"). Because we did not have site-level information about discrete seed bank vital rates, we simulated both the maximum and minimum possible standard deviations for each discrete vital rate. We then proceeded with two comparisons of vital rate variability and importance, once using the maximum possible discrete vital rate standard deviation, and another using the minimum. In order to determine the correlation between a single importance/variability value pair for discrete vital rates and a string of value pairs for continuous vital rate functions, we calculated mean importance and variability values for each continuous vital rate function. A

significant negative correlation between the mean or absolute scaled importance (logit VSS or elasticity) and mean or absolute variability (standard deviation of logit or log-transformed vital rates) across all vital rates would constitute support for the presence of vital rate buffering in this species (Fig. 1).

Asynchronous Responses and Source-Sink Dynamics*:* To determine whether *O. coloradensis* subpopulations showed asynchronous responses to environmental variation, we made a correlation matrix to determine how change in $\ln(\lambda)$ across each transition was correlated across each subpopulation, using values of $\ln(\lambda)$ derived from IPMs for each subpopulation (Table 2: IPMs "C"-"H"). We used the "mantel()" function from the vegan R package to perform a Mantel test, which determined if the Spearman correlation of $\ln(\lambda)$ across subpopulations was significantly related to the Euclidean distance between each subpopulation (Oksanen et al., 2020). A negative relationship between the distance between subpopulations and degree of correlation of $\ln(\lambda)$ would constitute evidence for spatial asynchrony between subpopulations (Fig. 1).

Because we did not have information about gene flow between subpopulations of *O. coloradensis* via pollination or seed dispersal, it was not possible to directly measure whether fine-scale source-sink dynamics were acting in these populations. However, because variation in population growth rate across space is a prerequisite for source-sink dynamics, the previously described tests for spatial asynchrony in subpopulations can also serve as a test for the pre-requisite spatial variation in λ underlying source-sink dynamics (Dibner et al., 2019). Again, this would be a negative relationship of distance between subpopulations and correlation of subpopulation $\ln(\lambda)$ (Fig. 1).

Results

Vital Rate Models

Larger non-reproductive plants were more likely to survive than smaller plants (Fig. 4A). Plants below ~7.5 cm were likely to be larger, while plants larger than ~7.5 cm were likely to be smaller the following year (Fig. 4B). Flowering probability was best approximated as a quadratic polynomial, where flowering probability peaked at 12 cm leaf length, and plants with the largest leaves exhibited low flowering probability (Fig. 4C). The number of seeds that a reproductive plant produced increased sharply with leaf size (Fig. 4D). The inclusion of additional covariates did not alter the overall shape or sign of the relationships between leaf size and vital rates, so models shown in Figure 4 did not include any additional covariates beyond leaf size.

Objective 1: Quantifying the Importance of the Seed Bank Stage

Integral Projection Models*:* We found that including a discrete seed bank stage in IPMs for *O. coloradensis* significantly increased the asymptotic population growth rate. The continuous state-only IPM (Table 2: IPM "A") predicted an asymptotic ln(λ) of 0.27 for all populations (95% CI: 0.269 - 0.271), while the continuous + discrete state IPM (Table 2: IPM "B") predicted an asymptotic ln(λ) of 0.65 (populations (95% CI: 0.648 - 0.650). All subsequent IPM results refer to models that included a discrete seed bank state.

The simplest two-state IPMs that excluded density dependence and environmental variation indicated that both the Soapstone prairie and FEWAFB populations had positive population growth rates (Table 2: Soapstone prairie- IPM "AA", ln(λ) = 0.50; FEWAFB – IPM "BB", ln(λ) = 0.73). The Diamond Creek subpopulation at FEWAFB had the highest population growth rate from 2018 to 2020 (Table 2: IPM "D", ln(λ) = 1.13), while the HQ3 subpopulation at Soapstone

prairie had the lowest growth rate (Table 2: IPM "G", $\ln(\lambda) = 0.395$). We parameterized multiple other sets of IPMs that used different combinations of covariates in their vital rate models, and almost all identified a positive population growth rate (Table 2).

A density-independent, discretized IPM kernel (made using IPM "B" in Table 2) showed transition probabilities within and between the discrete and continuous stages of the *O. coloradensis* life cycle when all populations and transitions were considered together (Fig. S2 A). Relative to the rest of the kernel, there was a very high probability that seeds stay in the seed bank, as well as a large contribution of seeds from medium-sized adult plants to the seed bank in the next year. The rates at which seeds are produced by adult plants and stay in the seed bank had the most impact on population growth rate (Fig. S2 C).

Objective 2: Evaluating Persistence Mechanisms

Negative Density Dependence*:* We found evidence that negative density- dependence was occurring in subpopulations of *O. coloradensis*. AIC comparison of continuous vital rate models indicate that density-dependent models are better predictors of the majority of vital rates than density-independent models in most subpopulations (Table 3). Models that included population size in the previous year as a covariate were better predictors of growth in five of six subpopulations. Density dependent models were better predictors of survival and seed production than density independent models in four out of six subpopulations, and density dependent models of flowering were better in one subpopulation. Recruit size distribution was not affected by density dependence—AIC model comparison did not indicate substantial differences, either negative or positive, between recruit size models with and without density dependence terms in any subpopulation. The vital rate models for the Meadow population at Soapstone Prairie were

455 least affected by density dependence. Although density dependence is important for *O.*
456 *coloradensis* in many situations, it appears only to be acting to decrease lambda at high density
457 (as in the highly dense Diamond Creek or HQ5 subpopulations), but not clearly increasing
458 lambda at low density (as in the sparsely populated Meadow subpopulation). We also found that,
459 within a subpopulation, population growth rate ($\ln(\lambda)$) was generally higher when subpopulation
460 size was smaller (Fig. 5 A). Similarly, there was a negative relationship within each
461 subpopulation between subpopulation size in year *t* and the ratio of subpopulation size in *t+1* to
462 subpopulation size in *t* (Fig. 5 B and D); Interestingly, these negative relationships were
463 generally pronounced at the subpopulation level, but were weak when examining data across all
464 subpopulations.

465 Demographic Compensation*:* Our analyses did not identify signatures of demographic
466 compensation in *O. coloradensis* populations. While there were negative correlations between
467 the effect of mean growing season temperature on vital rates for five combinations of vital rates,
468 none of these correlations were significant (Table 4). The only significant correlation was
469 positive. Ten thousand correlations of randomly assigned coefficients found that the number of
470 negative correlations in a matrix can be described by a normal distribution with a mean of 4.97
471 and a standard deviation of 1.60. Using this distribution as a null model, there was a 50.7%
472 probability of observing five negative correlations. The number of positive correlations in these
473 same ten thousand simulated matrices can be described by a normal distribution with a mean of
474 4.99 and a mean of 1.60. Using this distribution as a null model, there was a 50.1% probability of
475 observing five positive correlations. As such, there were not more negative or fewer positive
476 correlations than expected by chance. Although there was no significant evidence for
477 demographic compensation, it is notable that the effect of mean growing season temperature on

distribution of recruit size was negatively correlated with the effect of growing season temperature on all other vital rates. We were only able to compare coefficients across vital rate models for mean growing season temperature, because including precipitation and mean winter temperature as covariates resulted in overfitting in some vital rate models.

Vital Rate Buffering*:* We did not find evidence of vital rate buffering in the *O. coloradensis* populations we observed. Vital rate importance (either logit VSS or elasticity) and variability (corrected SD) were not significantly negatively correlated, regardless of the simulated standard deviation for discrete vital rates we used (Fig. 6; correlation with minimum discrete vital rate SD (**A**): $r = 0.43$, $P = 0.25$; correlation with maximum discrete vital rate SD (**B**): $r = -0.07$, $P = 0.85$). As a vital rate became more important for determining population growth rate, it did not become significantly less variable, showing no evidence that vital rate buffering is taking place (Fig. 1).

Asynchronous Responses and Source-Sink Dynamics*:* We did not identify a signature of asynchronous responses to environmental variation in *O. coloradensis* populations. There was not a significant relationship between the Spearman correlation of $\ln(\lambda)$ between subpopulations and their spatial proximity (Mantel statistic = 0.396, $P = 0.06$). We also performed Mantel tests using $\ln(\lambda)$ correlation and distance matrices calculated uniquely for each population. There was not a significant relationship between subpopulation growth rate and spatial proximity at either Soapstone prairie (Mantel statistic = -0.659, $P = 0.83$) or FEWAFB (Mantel statistic = 0.798, $P = 0.33$). While these tests did not identify significant relationships, we did find a positive relationship between correlation of $\ln(\lambda)$ and distance between subpopulations at Soapstone prairie, and a negative relationship between subpopulations at FEWAFB. Collectively, these

results fail to provide support for both asynchronous responses or the pre-requisite conditions underlying fine-scale source-sink dynamics in these *O. coloradensis* populations.

Discussion

Our demographic analysis of the two largest known populations of the globally rare *Oenothera coloradensis* evaluated the importance of seed banks to population dynamics and the demographic mechanisms that allow this rare species to persist. We found that including information about cryptic life stages alters the outcomes of the population model (Nguyen et al., 2019; Paniw et al., 2017), demonstrating the importance of accounting for this cryptic life stage in models used to inform management and conservation. We also found that *O. coloradensis* populations show signs of negative density- dependence at the subpopulation scale (Fig. 5; Table 3), but populations do not show substantial evidence of demographic compensation, vital rate buffering, spatial asynchrony, or the pre-requisite conditions for fine-scale source-sink dynamics. This may indicate that while certain of these mechanisms may be important for the persistence of small populations of rare plants in many cases, a species need not employ all of them to maintain a positive growth rate.

Including a discrete seed bank state in an IPM increased the asymptotic population growth rate compared to an IPM with only a continuous, size-based state, although both growth rates were still positive (Table 2: with seed bank: IPM "B", $\ln(\lambda) = 0.65$; without seed bank: IPM "A", $\ln(\lambda = 0.27)$. This increase in growth rate resulting from the inclusion of a seed bank in models indicates that the seed bank contributes to long-term population growth and thus persistence of this species. It also emphasizes that considering seed banks or other cryptic life stages in modeling efforts, while often difficult, could result in divergent model outcomes that in turn

would lead to qualitatively different conservation and management decisions. The importance of including the seed bank in the model was consistent with our expectations, and also aligns with the conventional notion that seed banks can act as buffers against stochastic causes of population decline. The discrete rates for the probability of persisting and transitioning out of the seed bank have high elasticity in the IPMs in which they are included, but not the highest elasticity of any vital rate (Fig. S2 C). The rate at which seeds produced by adult plants in year t go into the seed bank in year $t+1$ is the vital rate function with highest elasticity. Previous matrix population models of *O. coloradensis* without a seed bank state that were constructed in the 1990s identified the emergence rate of new seedlings as the vital rate most important for determining $\ln(\lambda)$ (Floyd & Ranker, 1998). Our finding that seed bank state transitions are important for this species aligns with this previous result, since rate of seedling emergence is the above-ground plant vital rate that is closest to the seed bank in this plant's life cycle. An important caveat to our comparison of models with and without seed bank stages is the fact that the seed bank vital rate parameters we used were inferred from laboratory tests of germination and viability rates, which may be imperfect representations of *in-situ* rates of viability and germination. The annual rate of seed death (10%) was inferred from an *in-situ* study, but is likely imprecise because of low sample size. Regardless of these potential sources of error, our results reinforce the fact that the seed bank can be an important element of a perennial plant's life cycle, and if possible, should be modeled explicitly based on *in-situ* estimates of the probability of seeds going into, persisting in, and emerging from the seed bank.

We found evidence that, of the five proposed demographic mechanisms of small population persistence, negative density dependence was the only one acting in these *O. coloradensis* populations. Including population size in the previous year as a covariate in vital rate models

typically improved model fit, suggesting that density dependence is an important driver of growth, survival, and reproduction (Table 3). Within a single subpopulation, population growth rate and the ratio of population size in year *t+1* to year *t* was generally higher when population size in year *t* was smaller (Fig. 5), which indicates that negative density dependence prevents subpopulations from crashing when their population size is very small. However, this pattern of higher growth rate at low population sizes did not exist when considering all subpopulations together (Fig. 5). This could indicate that each subpopulation is close to its carrying capacity for *O. coloradensis*, and that growth rate increases when the population size in a given subpopulation is small in comparison to its subpopulation-specific carrying capacity.

Oenothera coloradensis vital rates had correlated responses to variation in the abiotic environment (Table 4), which is the inverse of what is expected if demographic compensation is taking place. It is possible that a signal of vital rate buffering would appear if we considered different abiotic variables such as disturbance frequency or had more years of data encompassing a wider variation of environmental conditions, which may have allowed us to include more environmental covariates in models. However, of the environmental covariates we considered, the increased importance of growing season temperature as a driver of demographic rates relative to precipitation and winter temperature makes biological sense for this system. Winters in our study locations are routinely well below freezing, removing any possibility of growth during the winter season and ensuring the cold-stratification required for seed germination. Similarly, this species grows in a riparian habitat, which likely means they receive the water they require from growth from the water table and are not precipitation-limited. However, growing season temperature can fluctuate substantially from year to year at these study sites, and it makes sense that the effects of temperature, either direct or indirect, significantly impact vital rates in this

568 species. Even though the significance of these covariates aligns with the biological reality of this
569 system, the possibility still remains that with more data, evidence for demographic compensation
570 in this species would possibly emerge.

571 Vital rate buffering also was not identified, either with the minimum or maximum possible
572 simulated discrete vital rate variability (Fig. 6). Vital rates with higher variability (higher SD) did
573 not have a significantly higher or lower importance for determining $\ln(\lambda)$ in comparison to less
574 variable vital rates. This indicates that vital rate buffering is not stabilizing $\ln(\lambda)$ after abiotic or
575 demographic perturbation. The evidence for spatial asynchrony and fine-scale source-sink
576 dynamics was also not strong. Mantel tests did not identify a significant relationship between the
577 correlation of $\ln(\lambda)$ between subpopulations and their spatial proximity, but did identify non-
578 significant relationships between $\ln(\lambda)$ correlation and proximity. However, this relationship was
579 positive in Soapstone prairie subpopulations and negative in FEWAFB subpopulations, which
580 provides inconsistent support for these mechanisms. It is possible that, with the addition of
581 genetic evidence, we would find support for fine-scale source-sink dynamics. However, this
582 seems unlikely since we did not find evidence for the spatial variation of population growth
583 rate—a necessary pre-requisite for fine-scale source-sink dynamics acting as a persistence
584 mechanism.

585 It is somewhat surprising that negative density dependence is the only mechanism of small
586 population persistence that has significant support in these *O. coloradensis* populations, since
587 multiple mechanisms have been identified in at least one other rare species (Dibner et al., 2019).
588 It is possible that support for one or more of these persistence mechanisms could emerge if more
589 information about abiotic variation across space and time and data from more than three annual
590 transitions were available for analysis. One potential explanation for our finding support for only

one mechanism is that, while this species is a globally rare endemic with isolated subpopulations, it often is observed *in situ* growing at high local density. This strategy, which Rabinowitz describes as "locally abundant in a specific habitat but restricted geographically," may allow *O. coloradensis* to bypass the problems that small populations typically face, such as genetic and demographic bottlenecks that make them susceptible to stochastic environmental variation (Rabinowitz, 1981). It has also been shown that rare species are more likely than common species to benefit from facilitative interspecific interactions (Calatayud et al., 2020). *O. coloradensis* may participate in facilitative interactions with other species that increase its probability of persistence, although determining this will require further, community-level analysis. When compared to studies of persistence mechanisms in other species, our results illustrate the concept that species can employ distinct strategies for persistence (Rabinowitz, 1981). While demographic strategies that help maintain persistence may be effective for some species, other species may employ different strategies. This further emphasizes the importance of carefully considering the specific population and its community dynamics when managing and conserving rare species.

Our analysis of the population dynamics of *Oenothera coloradensis* at two distinct locations shows that this species has a life cycle that is strongly driven by introduction and persistence of seeds into a seed bank. More broadly, we show that this rare endemic species shows signs of negative density dependence. Populations of *O. coloradensis* may additionally be maintained via high local abundances that allow them to escape the challenges of small population size that rare species often face. In the context of this species, our results emphasize that successful management and conservation of *O. coloradensis* will require maintaining suitable microhabitat patches as well as conducting longer term monitoring to capture true changes in population size

614 rather than the short term "boom and bust cycles" that result from density dependence. More
615 broadly, these findings reinforce the importance of careful evaluation of the unique population
616 dynamics of rare species to inform successful conservation and management.

617 **References**

618 Abbott, R. E., Doak, D. F., & Peterson, M. L. (2017). Portfolio effects, climate change, and the
619 persistence of small populations: analyses on the rare plant *Saussurea weberi*. *Ecology*,
620 *98*(4), 1071–1081. https://doi.org/10.1002/ecy.1738
621 Arnoldi, J. F., Loreau, M., & Haegeman, B. (2019). The inherent multidimensionality of
622 temporal variability: how common and rare species shape stability patterns. *Ecology*
623 *Letters*, *22*(10), 1557–1567. https://doi.org/10.1111/ele.13345
624 Burgess, L. M. (2003). *Impacts of Mowing, Burning, and Climate on Germination and Seedling*
625 *Recruitment of Colorado Butterfly Plant (Gaura neomexicana* ssp. *coloradensis)*.
626 Masters Thesis -University of Wyoming, Laramie, WY.
627 Burgess, L. M., Hild, A. L., & Shaw, N. L. (2005). Capsule treatments to enhance seedling
628 emergence of *Gaura neomexicana* ssp. *coloradensis*. *Restoration Ecology*, *13*(1), 8–14.
629 https://doi.org/10.1111/j.1526-100X.2005.00002.x
630 Burner, R. C., Drag, L., Stephan, J. G., Birkemoe, T., Wetherbee, R., Muller, J., Siitonen, J.,
631 Snäll, T., Skarpaas, O., Potterf, M., Doerfler, I., Gossner, M. M., Schall, P., Weisser, W.
632 W., & Sverdrup-Thygeson, A. (2022). Functional structure of European forest beetle
633 communities is enhanced by rare species. *Biological Conservation*, *267*(June 2021).
634 https://doi.org/10.1016/j.biocon.2022.109491
635 Calatayud, J., Andivia, E., Escudero, A., Melián, C. J., Bernardo-Madrid, R., Stoffel, M.,
636 Aponte, C., Medina, N. G., Molina-Venegas, R., Arnan, X., Rosvall, M., Neuman, M.,

637 Noriega, J. A., Alves-Martins, F., Draper, I., Luzuriaga, A., Ballesteros-Cánovas, J. A.,
638 Morales-Molino, C., Ferrandis, P., … Madrigal-González, J. (2020). Positive associations
639 among rare species and their persistence in ecological assemblages. *Nature Ecology and*
640 *Evolution*, *4*(1), 40–45. https://doi.org/10.1038/s41559-019-1053-5
641 Caswell, H. (2001). *Matrix Population Models: Construction, Analysis, and Interpretation* (2nd
642 ed.). Sinauer Associates.
643 Dibner, R. R., Peterson, M. L., Louthan, A. M., & Doak, D. F. (2019). Multiple mechanisms
644 confer stability to isolated populations of a rare endemic plant. *Ecological Monographs*,
645 *89*(2), 1–16. https://doi.org/10.1002/ecm.1360
646 Drury, W. H. (1974). Rare species. *Biological Conservation*, *6*(3), 162–169.
647 https://doi.org/10.1016/0006-3207(74)90061-5
648 Easterling, M. R., Ellner, S. P., & Dixon, P. M. (2000). Size-Specific Sensitivity: Applying a
649 New Structured Population Model. *Ecology*, *81*(3), 694–708.
650 https://doi.org/10.1890/0012-9658(2000)081[0694:SSSAAN]2.0.CO;2
651 Ellner, S. P., Childs, D. Z., & Rees, M. (2016). *Data-driven Modelling of Structured*
652 *Populations*. Springer International Publishing. https://doi.org/10.1007/978-3-319-28893-
653 2
654 Ellner, S. P., & Rees, M. (2006). Integral projection models for species with complex
655 demography. *The American Naturalist*, *167*(3), 410–428. https://doi.org/10.1086/499438
656 Enquist, B. J., Feng, X., Boyle, B., Maitner, B., Newman, E. A., Jørgensen, P. M., Roehrdanz, P.
657 R., Thiers, B. M., Burger, J. R., Corlett, R. T., Couvreur, T. L. P., Dauby, G., Donoghue,
658 J. C., Foden, W., Lovett, J. C., Marquet, P. A., Merow, C., Midgley, G., Morueta-Holme,
659 N., … McGill, B. J. (2019). The commonness of rarity: Global and future distribution of

660 rarity across land plants. *Science Advances*, *5*(11), 1–14.
661 https://doi.org/10.1126/sciadv.aaz0414
662 Fertig, W. (2000). *Status Review of the Colorado Butterfly Plant (Gaura neomexicana* ssp.
663 *coloradensis)*. Prepared for the Wyoming Cooperative Fish and Wildlife Research Unit,
664 US Fish and Wildlife Service, and Wyoming Game and Fish Department by the
665 Wyoming Natural Diversity Database.
666 Fieberg, J. R., Vitense, K., & Johnson, D. H. (2020). Resampling-based methods for biologists.
667 *PeerJ*, *2020*(3). https://doi.org/10.7717/peerj.9089
668 Floyd, S. K., & Ranker, T. A. (1998). Analysis of a Transition Matrix Model for *Gaura*
669 *neomexicana* ssp. *coloradensis* (Onagraceae) Reveals Spatial and Temporal
670 Demographic Variability. *International Journal of Plant Sciences*, *159*(5), 853–863.
671 Gaillard, J.-M., & Yoccoz, N. G. (2003). Temporal variation in survival of mammals: A case of
672 environmental canalization? *Ecology*, *84*(12), 3294–3306. https://doi.org/10.1890/02-
673 0409
674 Heidel, B., Tuthill, D., & Wallace, Z. (2021). *33-Year Population Trends of Colorado Butterfly*
675 *Plant (Oenothera coloradensis; Onagraceae), a Short-Lived Riparian Species on F. E.*
676 *Warren Air Force Base, Laramie County, Wyoming*. Prepared for U.S. Fish and Wildlife
677 Service and F. E. Warren Air Force Base by the Wyoming Natural Diversity Database.
678 Hilde, C. H., Gamelon, M., Sæther, B.-E., Gaillard, J.-M., Yoccoz, N. G., & Pélabon, C. (2020).
679 The Demographic Buffering Hypothesis: Evidence and Challenges. *Trends in Ecology &*
680 *Evolution*, *35*(6), 523–538. https://doi.org/10.1016/j.tree.2020.02.004

Jongejans, E., Sheppard, A. W., & Shea, K. (2006). What controls the population dynamics of the invasive thistle *Carduus nutans* in its native range? *The Journal of Applied Ecology*, *43*(5), 877–886. https://doi.org/10.1111/j.1365-2664.2006.01228.x

Kauffman, M. J., Pollock, J. F., & Walton, B. (2004). Spatial structure, dispersal, and management of a recovering raptor population. *The American Naturalist*, *164*(5), 582–597. https://doi.org/10.1086/424763

Leitão, R. P., Zuanon, J., Villéger, S., Williams, S. E., Baraloto, C., Fortune, C., Mendonça, F. P., & Mouillot, D. (2016). Rare species contribute disproportionately to the functional structure of species assemblages. *Proceedings of the Royal Society B: Biological Sciences*, *283*(1828). https://doi.org/10.1098/rspb.2016.0084

Levin, S. C., Childs, D. Z., Compagnoni, A., Evers, S., Knight, T. M., & Salguero-Gómez, R. (2021). ipmr: Flexible implementation of Integral Projection Models in R. *Methods in Ecology and Evolution*, *12*(10), 1826–1834. https://doi.org/10.1111/2041-210X.13683

Levins, R., & Culver, D. (1971). Regional Coexistence of Species and Competition between Rare Species. *Proceedings of the National Academy of Sciences*, *68*(6), 1246–1248. https://doi.org/10.1073/pnas.68.6.1246

Lyons, K. G., Brigham, C. A., Traut, B. H., & Schwartz, M. W. (2005). Rare species and ecosystem functioning. *Conservation Biology: The Journal of the Society for Conservation Biology*, *19*(4), 1019–1024. https://doi.org/10.1111/j.1523-1739.2005.00106.x

Magurran, A. E., & Henderson, P. A. (2011). Commonness and Rarity. In A. E. Magurran & B. J. McGill (Eds.), *Biological diversity : frontiers in measurement and assessment* (pp. 97–104). Oxford University Press. https://www.researchgate.net/publication/281461811

May, R. M. (1973). Stability in Randomly Fluctuating Versus Deterministic Environments. *The American Naturalist*, *107*(957), 621–650.

McDonald, J. L., Franco, M., Townley, S., Ezard, T. H. G., Jelbert, K., & Hodgson, D. J. (2017). Divergent demographic strategies of plants in variable environments. *Nature Ecology and Evolution*, *1*(2). https://doi.org/10.1038/s41559-016-0029

Merow, C., Dahlgren, J. P., Metcalf, C. J. E., Childs, D. Z., Evans, M. E. K., Jongejans, E., Record, S., Rees, M., Salguero-Gómez, R., & Mcmahon, S. M. (2014). Advancing population ecology with integral projection models: A practical guide. *Methods in Ecology and Evolution*, *5*(2), 99–110. https://doi.org/10.1111/2041-210X.12146

Morris, W. F., & Doak, D. F. (2002). *Quantitative Conservation Biology: Theory and Practice of Population Viability Analysis*. Sinauer Associates.

Munk, L. M., Hild, A. L., & Whitson, T. D. (2002). Rosette recruitment of a rare endemic forb (*Gaura neomexicana* subsp. *coloradensis*) with canopy removal of associated species. *Restoration Ecology*, *10*(1), 122–128. https://doi.org/10.1046/j.1526-100X.2002.10113.x

Nei, M., Maruyama, T., & Chakraborty, R. (1975). The Bottleneck Effect and Genetic Variability in Populations. *Evolution; International Journal of Organic Evolution*, *29*(1), 1–10.

Nguyen, V., Buckley, Y. M., Salguero-Gómez, R., & Wardle, G. M. (2019). Consequences of neglecting cryptic life stages from demographic models. *Ecological Modelling*, *408*(June). https://doi.org/10.1016/j.ecolmodel.2019.108723

Oksanen, J., Blanchet, F. G., Friendly, M., Kindt, R., Legendre, P., McGlinn, D., Minchin, P. R., O'Hara, R. B., Simpson, G. L., Solymos, P., Stevens, M. H. H., Szoecs, E., & Wagner, H.

(2020). *vegan: Community Ecology Package*. R package version 2.5-7. https://cran.r-project.org/package=vegan

Paniw, M., Quintana-Ascencio, P. F., Ojeda, F., & Salguero-Gómez, R. (2017). Accounting for uncertainty in dormant life stages in stochastic demographic models. *Oikos* , *126*(6), 900–909. https://doi.org/10.1111/oik.03696

Pfister, C. A. (1998). Patterns of variance in stage-structured populations : Evolutionary predictions and ecological implications. *Proceedings of the National Academy of Sciences*, *95*(January), 213–218.

PRISM Climate Group; Oregon State University. (2021). *PRISM Climate Group, Oregon State University*. https://prism.oregonstate.edu

Pulliam, H. R. (2016). *Sources , Sinks , and Population Regulation* (Vol. 132, pp. 652–661). The University of Chicago Press for The American Society of Naturalists.

Rabinowitz, D. (1981). Seven forms of rarity. In H. Synge (Ed.), *The Biological aspects of rare plant conservation*. John WIley & Sons, Ltd. https://doi.org/10.2307/4110060

Ramula, S., Rees, M., & Buckley, Y. M. (2009). Integral projection models perform better for small demographic data sets than matrix population models: A case study of two perennial herbs. *The Journal of Applied Ecology*, *46*(5), 1048–1053. https://doi.org/10.1111/j.1365-2664.2009.01706.x

Rees, M., Childs, D. Z., Metcalf, C. J. E., Rose, K. E., Sheppard, A. W., & Grubb, P. J. (2006). Seed dormancy and delayed flowering in monocarpic plants: selective interactions in a stochastic environment. *The American Naturalist*, *168*(2), E53–E71. https://doi.org/10.1086/505762

748 Rosenzweig, M. L., & Lomolino, M. V. (1997). The Biology of Rarity. In W. E. Kunin & K. J.
749 Gaston (Eds.), *The Biology of Rarity*. Chapman & Hall. https://doi.org/10.1007/978-94-
750 011-5874-9_7
751 Rovere, J., & Fox, J. W. (2019). Persistently rare species experience stronger negative frequency
752 dependence than common species: A statistical attractor that is hard to avoid. *Global*
753 *Ecology and Biogeography: A Journal of Macroecology*, *28*(4), 508–520.
754 https://doi.org/10.1111/geb.12871
755 Säterberg, T., Jonsson, T., Yearsley, J., Berg, S., & Ebenman, B. (2019). A potential role for rare
756 species in ecosystem dynamics. *Scientific Reports*, *9*(1), 11107.
757 https://doi.org/10.1038/s41598-019-47541-6
758 Sgarbi, L. F., & Melo, A. S. (2018). You don't belong here: explaining the excess of rare species
759 in terms of habitat, space and time. *Oikos* , *127*(4), 497–506.
760 https://doi.org/10.1111/oik.04855
761 Spear, M. J., Walsh, J. R., Ricciardi, A., & Vander Zanden, M. J. (2021). The Invasion Ecology
762 of Sleeper Populations: Prevalence, Persistence, and Abrupt Shifts. In *BioScience* (Vol.
763 71, Issue 4, pp. 357–369). Oxford University Press.
764 https://doi.org/10.1093/biosci/biaa168
765 Stanley, S. M. (1979). *Macroevolution: Pattern and Process*. W. H. Freeman.
766 Tuljapurkar, S. (1989). An Uncertain Life : Demography in Random Environments. *Theoretical*
767 *Population Biology*, *35*(3), 227–294.
768 U.S. Fish & Wildlife Service. Endangered and threatened wildlife and plants: removing
769 *Oenothera coloradensis* (colorado butterfly plant) from the federal list of endangered and
770 threatened plants. (2019). 50 C.F.R. pt. 17.

https://www.federalregister.gov/documents/2019/11/05/2019-24124/endangered-and-threatened-wildlife-and-plants-removing-oenothera-coloradensis-colorado-butterfly

U.S. Fish & Wildlife Service. Endangered and threatened wildlife and plants: Threatened status for the colorado butterfly plant (*Gaura neomexicana* ssp. coloradensis) from southeastern Wyoming, northcentral colorado, and extreme western Nebraska. (2000). 50 C.F.R. pt. 17. https://www.federalregister.gov/documents/2000/10/18/00-26544/endangered-and-threatened-wildlife-and-plants-threatened-status-for-the-colorado-butterfly-plant

Villellas, J., Doak, D. F., García, M. B., & Morris, W. F. (2015). Demographic compensation among populations: What is it, how does it arise and what are its implications? *Ecology Letters*, *18*(11), 1139–1152. https://doi.org/10.1111/ele.12505

Vincent, H., Bornand, C. N., Kempel, A., & Fischer, M. (2020). Rare species perform worse than widespread species under changed climate. *Biological Conservation*, *246*, 108586. https://doi.org/10.1016/j.biocon.2020.108586

Vitalis, R., Glémin, S., & Olivieri, I. (2004). When genes go to sleep: The population genetic consequences of seed dormancy and monocarpic perenniality. *The American Naturalist*, *163*(2), 295–311. https://doi.org/10.1086/381041

Wagner, W. L., Krakos, K. N., & Hoch, P. C. (2013). Taxonomic changes in *Oenothera* sections *Gaura* and *Calylophus* (Onagraceae). *PhytoKeys*, *28*, 61–72. https://doi.org/10.3897/phytokeys.28.6143

William A Link, Paul F Doherty, Fr. (2002). Scaling in sensitivity analysis. *Ecology*, *83*(12), 3299–3305. https://doi.org/10.1890/0012-9658(2002)083[3299:SISA]2.0.CO;2

Williams, J. L., Miller, T. E. X., & Ellner, S. P. (2012). Avoiding unintentional eviction from integral projection models. *Ecology*, *93*(9), 2008–2014. https://doi.org/10.1890/11-2147.1

Figures

Figure 1:

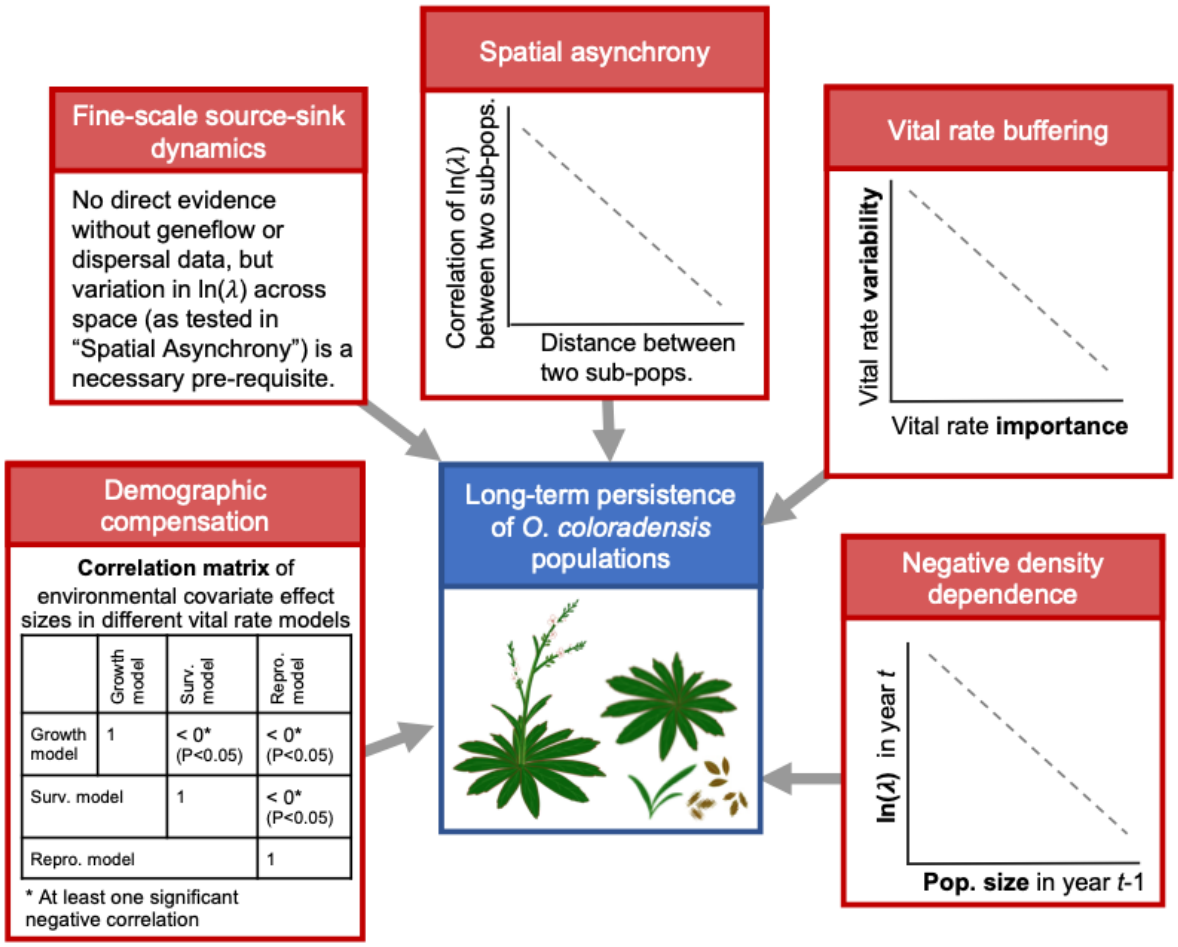

798 Figure 2:

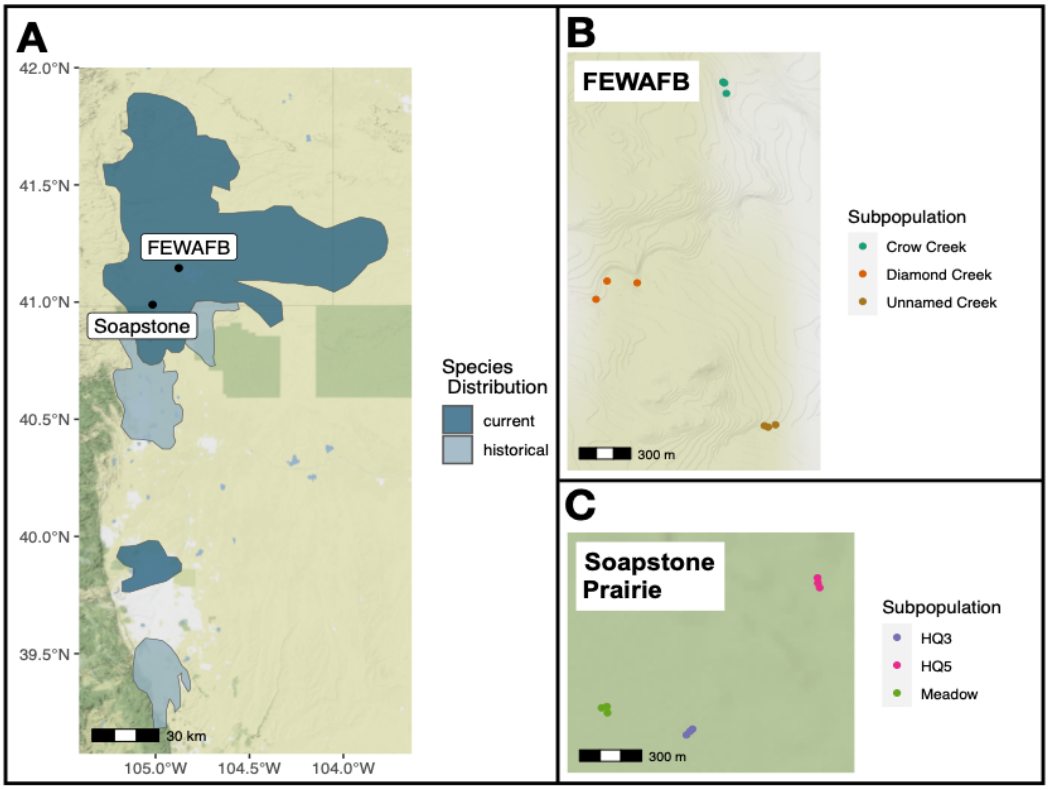

799

800

801 Figure 3:

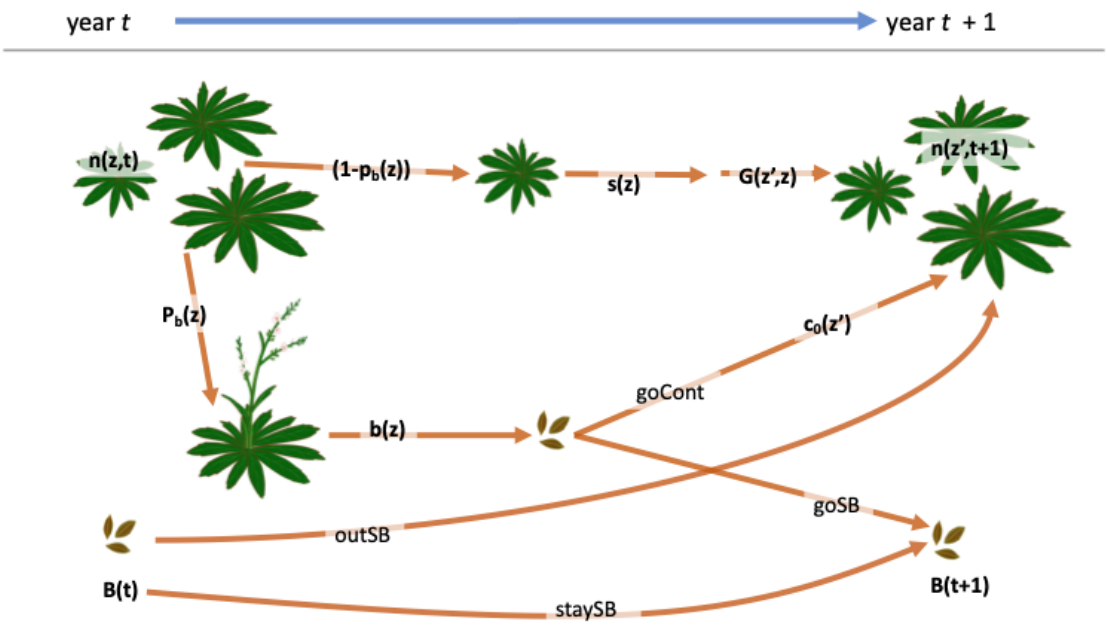

802

803 Figure 4:

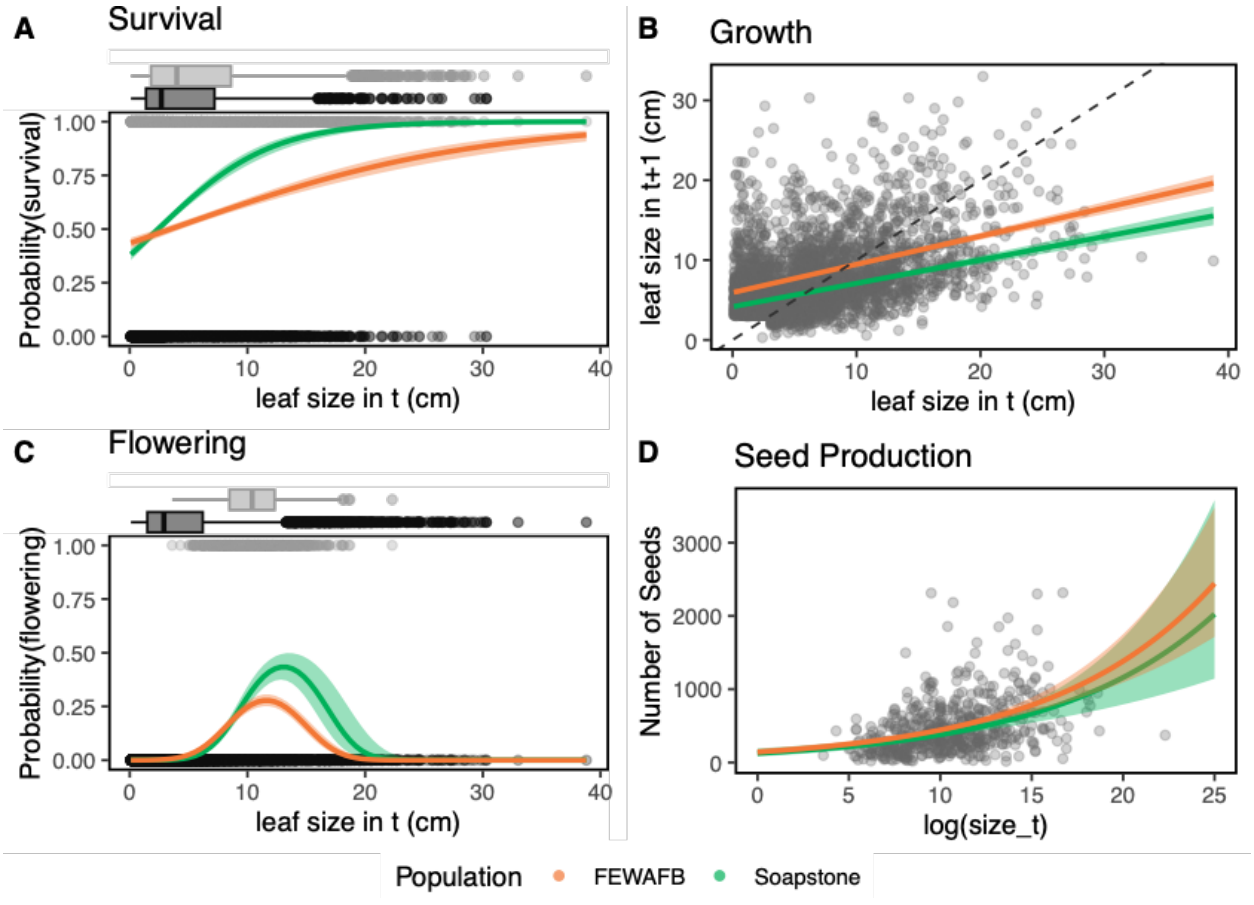

804

805

806 Figure 5:

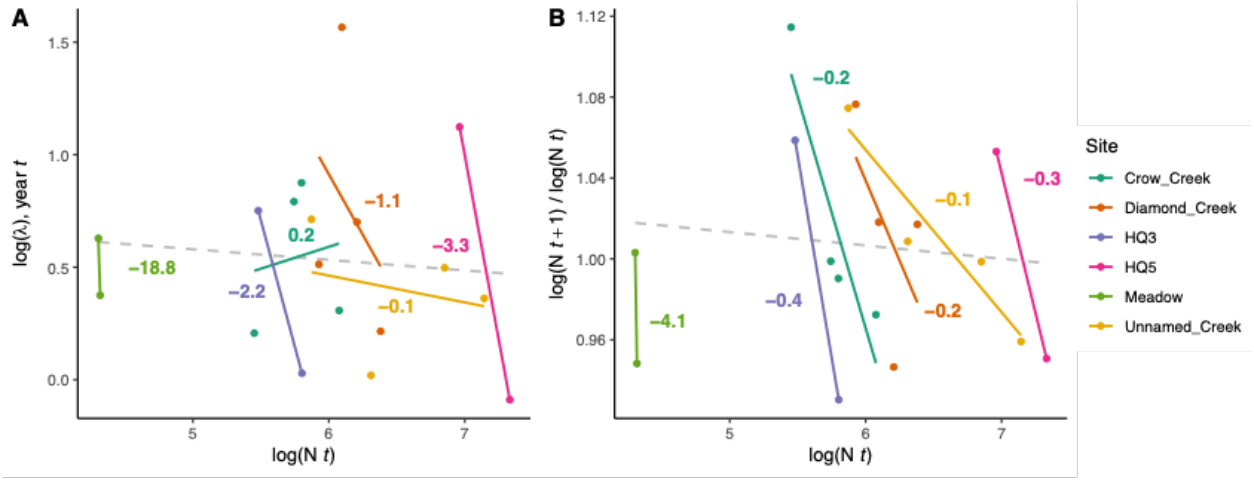

807

808

809 Figure 6:

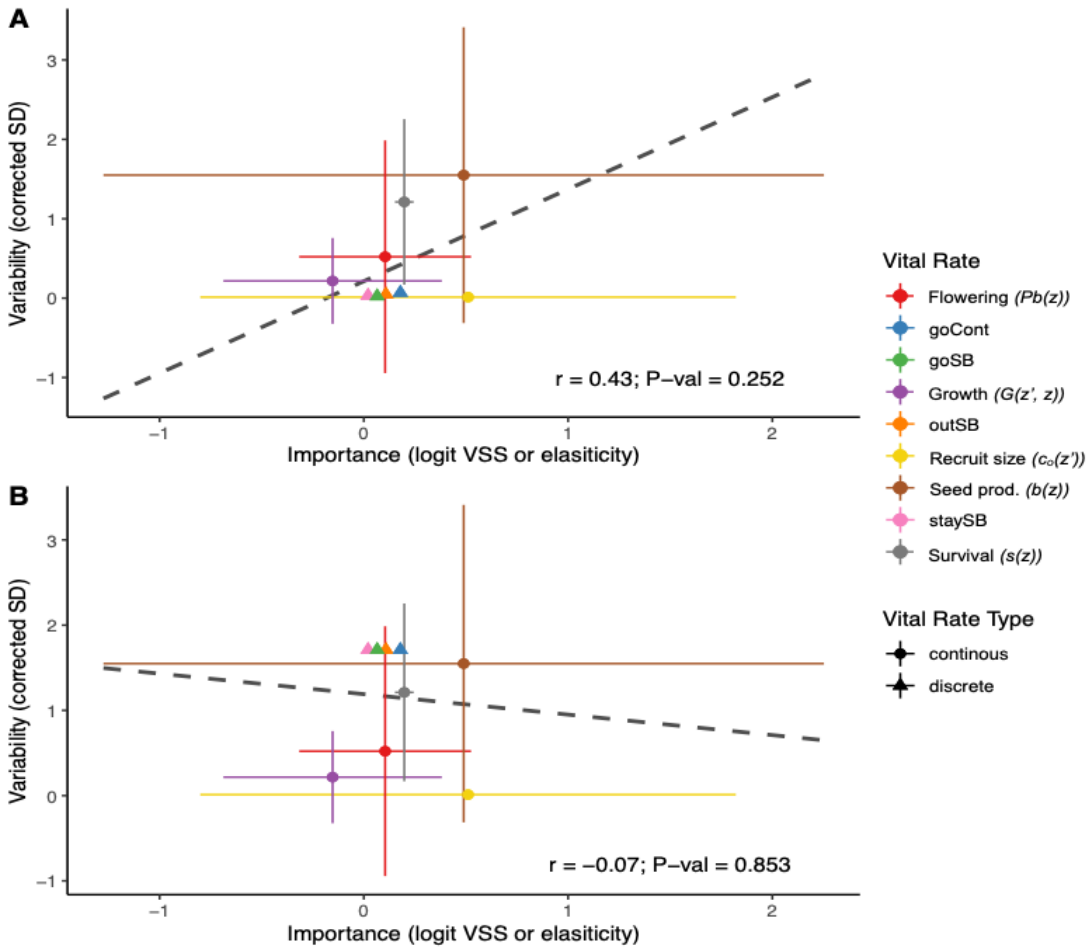

810

811
812

Figure Captions

Figure 1. The evidence that would be required to show support for each of the five mechanisms that can contribute to the long-term viability of small populations of rare species.

Figure 2: (**A**) The current known distribution of *O. coloradensis*, shown in dark blue, extends into Wyoming, Colorado, and Nebraska. The historical distribution included the current distribution area as well as some additional locations shown in pale blue. Distribution information comes from Everson, 2019. Black dots show the relative location of the FEWAFB and Soapstone prairie populations included in this study. Colored dots show the location of plots in each subpopulation at FEWAFB (**B**) and Soapstone Prairie (**C**).

Figure 3. Diagram of the *O. coloradensis* life-cycle, with transitions labeled with the notation used in vital equations that are described in detail in Table 1. Based on model structures and notation from: (Ellner et al., 2016; Merow et al., 2014; Paniw et al., 2017).

Figure 4. The effect of current year leaf size on vital rates in monitored *O. coloradensis* populations. Data from all sites and all transitions is shown. Lines indicate vital rate functions for each population, and include only size as a predictor, with the exception of flowering models, which include a (size term. Bands around each line show 95% confidence intervals. In plots A & C, boxplots above the main panels indicate the distribution of leaf size for individuals that did not survive or flower (dark grey) or did survive or flower (light grey). Grey points indicate data for an individual plant in a given transition. The dashed line in panel B shows a 1:1 line. The sharp cut-off in size in panel B is due to the fact that two-year-old plants could not be seedlings, which were classified as any plant less than 3 cm in size. Note that while leaf size in cm is shown in these plots for ease of interpretation, these values have been back-transformed from the ln(leaf size) values that were used in models.

Figure 5. Both analyses we employed demonstrated support for negative density dependence in the populations we studied. **A**) Within the same subpopulation, each indicated by a different color, population growth rate ($\ln(\lambda)$) calculated from IPMs decreased as population size ($\ln(N_t)$) increased. (**B**) Additionally, within each subpopulation, population growth rate calculated by change in population size from year *t* to year *t+1* ($\ln(N_{t+1}/\ln(N_t)$) also decreased as population size increased. In **A** and **B**, each point represents values calculated from models using data from one transition in one subpopulation. Solid lines show linear regressions of the relationships between $\ln(N_t)$ and the respective response variable in each subpopulation. Numbers adjacent to these solid lines show the slope of each relationship, and are color-coded by subpopulation. Dashed gray lines show linear regressions of the relationships between ($\ln(N_t)$) and the respective response variable across all subpopulations.

Figure 6. The relationship between the variability of each vital rate (measured by corrected standard deviation) and its importance (measured by logit VSS (logit variance stabilized sensitivity) or elasticity) does not show support for vital rate buffering. In these figures, a triangle indicates importance and variability for a discrete vital rate parameter, while a circle indicates the mean of importance and variability across an entire continuous vital rate function. Colors in the figure correspond to each vital rate, which are further defined in Table 1. Error bars around continuous vital rate means span the 5^{th} to 95^{th} percentiles of either importance or variability values calculated for an entire continuous vital rate function. Dashed lines show the correlation between (mean) variability and (mean) importance across all vital rates. Because we

lacked data to calculate the actual standard deviation of discrete vital rates, we simulated both the minimum and maximum possible standard deviation for each of these rates. (**A**) With the minimum possible discrete vital rate variability, there is a positive but insignificant correlation between vital rate variability and importance (r = 0.43, $P = 0.25$). (**B**) Using the maximum possible discrete vital rate variability, there is a negative but insignificant correlation between vital rate variability and importance (r = -0.07, $P = 0.85$).

865 **Tables**

866 Table 1

Vital Rate	Description	Model
pEstab	*P*(seed produced in t establishes as a seedling in t+1)	$pEstab = \frac{(Num.\ new\ recruits\ in\ year_{t+1})}{Num.\ seeds\ produced\ in\ year_t}$
goCont	*P*(seed produced in *t* germinates in *t+1*)	$goCont = viab.rate \times germ.rate$
outSB	*P*(seed bank seed in *t* germinates in *t+1*)	$outSB = germ.rate\ (1 - death\ rate)$
goSB	*P*(seed produced in *t* goes into the seed bank in *t+1*)	$goSB = viab.rate(1 - germ.rate)$
staySB	*P*(seed bank seed in *t* stays in the seed bank in *t+1*)	$staySB = (1 - germ.rate) \times (1 - death\ rate)$
Survival *(s(z))*	*P*(survival from *t* to *t+1*)	$logit(survival) \sim \beta_0 + \beta_1(\ln(size_t)) + \epsilon$
Flowering *(Pb(z))*	*P*(flowering in *t*)	$logit(flowering) \sim \beta_0 + \beta_1(\ln(\text{size}_t)) + \beta_2(\ln(\text{size}_t)^2) + \epsilon$
Seed prod. *(b(z))*	Seed production in *t*	$exp(seed\ number) \sim \beta_0 + \beta_1(\ln(size_t)) + \epsilon$
Growth *(G(z',z))*	Distribution of longest leaf size in year *t*	$G(z', z) = N(\mu_s, \sigma_s);$ $\mu_s \sim \beta_0 + \beta_1(\ln(size_t)) + \epsilon;$ $\sigma_s \sim RSE(\beta_0 + \beta_1(\ln(size_t)) + \epsilon)$
Recruit size *($c_o(z')$)*	Distribution of new recruit size in year *t*	$c_o(z') = N(\mu_r, \sigma_r);$ $\mu_r = mean(size\ of\ recruits\ in\ year_t);$ $\sigma_r = stnd.dev.(size\ of\ recruits\ in\ year_t);$

*RSE = residual standard error

867
868

869 Table 2:

IPM	Data Included														Transition		Covariates		ln(λ) (95% CI)
	Continuous State Only	Continuous + Seed Bank State	All subpopulations	Each pop.		Each subpop.									All Transitions	2018-2019 2019-2020	Density dependence	Environmental Covariates	
				Soapstone	FEWAFB	Unnamed Creek	Diamond Creek	Crow Creek	Meadow	HQ3	HQ5								
A	x		x												x				0.27 (0.269, 0.271)
B		x	x												x				0.65 (0.648, 0.650)
C		x				x									x				0.48 (0.477, 0.489)
D		x					x								x				1.13 (1.124, 1.142)
E		x						x							x				0.74 (0.725, 0.746)
F		x							x						x				0.54 (0.520, 0.551)
G		x								x					x				0.395 (0.378, 0.401)
H		x									x				x				0.53 (0.526, 0.540)
I		x				x									x		x		0.59† (0.576, 0.637)
J		x					x								x		x		0.63† (0.611, 0.723)
K		x						x							x		x		−0.10† (−0.135, 0.063)
L		x							x						x		x		−0.20† (−0.229, −0.167)
M		x								x					x		x		1.31† (1.294, 1.354)
N		x									x				x		x		2.31† (2.297, 2.33)
S		x				x									x		x	x	0.58†
T		x					x								x		x	x	0.51†
U		x						x							x		x	x	0.90†
V		x							x						x		x	x	-0.27†

IPM	Data Included															Transition		Covariates		ln(λ) (95% CI)
	Continuous State Only	Continuous + Seed Bank State	All subpopulations	Each pop.		Each subpop.										All Transitions	2018-2019	2019-2020	Density dependence	Environmental Covariates	
				Soapstone	FEWAFB	Unnamed Creek	Diamond Creek	Crow Creek	Meadow	HQ3	HQ5										
W	x									x						x			x	x	-0.18 †
X	x										x					x			x	x	0.76†
AA	x			x												x					0.50 (0.497, 0.501)
BB	x				x											x					0.73 (0.729, 0.733)
CC	x					x											x				0.38 (0.370, 0.388)
DD	x						x										x				1.56 (1.545, 1.572)
EE	x							x									x				0.90 (0.864, 0.904)
FF	x								x								x				0.62 (0.592, 0.637)
GG	x									x							x				0.73 (0.727, 0.753)
HH	x										x						x				1.11 (1.108, 1.126)
II	x					x												x			0.50 (0.492, 0.513)
JJ	x						x											x			0.71 (0.692, 0.726)
KK	x							x										x			0.76 (0.739, 0.774)
LL	x								x									x			0.41 (0.378, 0.448)
MM	x									x								x			0.03 (0.013, 0.040)
NN	x										x							x			-0.10 (-0.112, -0.097)

*Note: We did not calculate bootstrap 95% confidence intervals for ln(λ) of models "S" –"X", since only vital rate parameters and not lambda values from these models were used in further analysis.

†: These values show stochastic lambda ($ln(\lambda_s)$). Other values are asymptotic lambda ($ln(\lambda_a)$).

870 Table 3:

Vital Rate Model		Subpopulation					
		Crow Creek	Diamond Creek	Unnamed Creek	HQ5	HQ3	Meadow
Survival	DI	776.58	1012.68	2684.34	3242.63	716.66	166.13
	DD	757.84	905.39	26848.74	2922.91	637.84	166.83
	ΔAIC	**18.74**	**107.28**	-0.41	**320.33**	**78.82**	-0.70
Growth	DI	510.34	953.29	1098.95	1570.93	300.18	116.54
	DD	506.61	931.15	1068.14	1112.78	269.73	113.88
	ΔAIC	**3.73**	**22.15**	**30.811**	**458.15**	**30.45**	2.66
Flowering	DI	371.68	523.30	1087.93	538.52	191.46	104.24
	DD	373.31	523.74	1087.48	483.99	193.22	106.96
	ΔAIC	-1.63	-0.44	0.45	**54.52**	-1.76	-1.72
Seed production	DI	842.00	1580.85	2815.89	1423.02	598.75	280.09
	DD	835.59	1566.83	2817.19	1419.32	594.63	281.45
	ΔAIC	**6.41**	**14.02**	-1.29	**3.71**	**4.12**	-1.35
Recruit size	DI	921.31	1028.23	3378.43	4629.87	967.83	173.03
	DD	923.24	1026.63	3380.53	4631.84	969.06	175.02
	ΔAIC	-1.93	1.61	-1.93	-1.97	-1.23	-1.99

871

872 Table 4:

	Vital Rate				
	Flowering	*Survival*	*Growth*	*Seed Prod.*	*Recruit Size*
Flowering	1.00 (0)	0.474 (0.342)	0.136 (0.797)	-0.073 (0.890)	-0.786 (0.064)
Survival		1.00 (0)	0.886 **(0.019)**	0.675 (0.141)	-0.3570 (0.237)
Growth			1.00 (0)	0.664 (0.150)	-0.270 (0.606)
Seed Prod.				1.00 (0)	-0.432 (0.393)
Recruit Size					1.00 (0)

873
874

875 **Table Captions**
876
877 Table 1. Description of vital rates used in IPMs.

878 Table 2. A description of the data used to create each IPM, as well as the covariates included in
879 the vital rate models used in that IPM. ln(λ) estimates and 95% bootstrap confidence intervals of
880 ln(λ) are also shown for each IPM.

881 Table 3. Comparison of vital rate models that do and do not include density dependence. The
882 "DI" and "DD" rows contain AIC values for each vital rate model in each subpopulation for
883 models that are density-independent (DI) and density-dependent (DD). The difference between
884 the AIC of DI and DD models is shown in the ΔAIC row. Bold text indicates that the |ΔAIC|
885 value is > 3, which means that including a term for density dependence substantially changed
886 that vital rate model. A positive |ΔAIC| indicates that including density dependence improved the
887 model, while a negative value indicates that including density dependence made model fit worse.

888 Table 4. Spearman correlations between mean growing season temperature coefficients in each
889 continuous vital rate function. Below each correlation value is the P value for that correlation.
890 Bold text indicates a significant correlation.